A Transient Intermediate in the Reaction Catalyzed by (*S*)-Mandelate Dehydrogenase from *Pseudomonas putida*†

Asteriani R. Dewanti and Bharati Mitra*

Department of Biochemistry and Molecular Biology, School of Medicine, Wayne State University, Detroit, Michigan 48201

Received July 30, 2003; Revised Manuscript Received September 11, 2003

ABSTRACT: (*S*)-Mandelate dehydrogenase from *Pseudomonas putida* is a member of a FMN-dependent enzyme family that oxidizes (*S*)-α-hydroxyacids to α-ketoacids. The reductive half-reaction consists of the steps involved in substrate oxidation and FMN reduction. In this study, we investigated the mechanism of this half-reaction in detail. At low temperatures, a transient intermediate was formed in the course of the FMN reduction reaction. This intermediate is characteristic of a charge-transfer complex of oxidized FMN and an electron-rich donor and is formed prior to full reduction of the flavin. The intermediate was not due to binding of anionic substrates or inhibitors. It was only observed with efficient substrates that have high k_{cat} values. At higher temperatures, it was formed within the dead time of the stopped-flow instrument. The rate of formation of the intermediate was 3−4-fold faster than its rate of disappearance; the former had a larger isotope effect. This suggests that the charge-transfer donor is an electron-rich carbanion/enolate intermediate that is generated by the base-catalyzed abstraction of the substrate α-proton. This is consistent with the observation that the intermediate was not observed with the R277K and R277G mutants, which have been shown to destabilize the carbanion intermediate (Lehoux, I. E., and Mitra, B. (2000) *Biochemistry 39,* 10055−10065). Thus, the MDH reaction has two rate-limiting steps of similar activation energies: the formation and breakdown of a distinct intermediate, with the latter step being slightly more rate limiting. We also show that MDH is capable of catalyzing the reverse reaction, the reoxidation of reduced MDH by the product ketoacid, benzoylformate. The transient intermediate was observed during the reverse reaction as well, confirming that it is indeed a true intermediate in the MDH reaction pathway.

(*S*)-Mandelate dehydrogenase (MDH),[1] an enzyme in the mandelate metabolic pathway in *Pseudomonas putida* (ATCC 12633), catalyzes the oxidation of (*S*)-mandelate to benzoylformate (*1*).

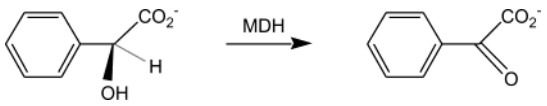

MDH is a member of a family of FMN-dependent α-hydroxyacid dehydrogenases/oxidases, which specifically oxidizes the (*S*)-enantiomer of α-hydroxyacids to α-ketoacids (*2*, *3*). The members of this family share extensive sequence similarity. In addition, three-dimensional structural comparisons of glycolate oxidase from spinach, flavocytochrome b_2 (L-lactate dehydrogenase) from *Saccharomyces cerevisiae*, and a soluble form of the membrane-bound MDH indicate that the enzymes have similar structures and identical active site geometries (*4*−*7*). Thus, it is likely that the reductive half-reaction, involving oxidation of the α-hydroxyacid to α-ketoacid and the reduction of FMN, is likely to proceed through the same mechanism for all these enzymes (*4*−*7*). The second half-reaction involving reoxidation of the reduced FMN is different for the various enzymes. Unlike the oxidases, the dehydrogenases do not react with molecular oxygen. The flavocytochrome b_2s react with an intramolecular heme, whereas the bacterial membrane-bound dehydrogenases, including MDH, transfer the electrons to a component of the electron transport chain.

Biochemical studies for a number of enzymes in this family support a mechanism in which the oxidation of the α-hydroxyacid anion proceeds stepwise through a carbanion intermediate (*8*−*10*). Structural analyses of glycolate oxidase, flavocytochrome b_2, and MDH are compatible with this mechanism (*6*, *7*, *11*). A conserved histidine residue (His274 in MDH) is suitably positioned to abstract the α-proton from the substrate, resulting in the formation of a highly charged carbanion intermediate (*12*). The carbanion is stabilized by two conserved arginine residues (Arg165 and Arg277 in MDH) that interact with the substrate carboxylate group (*13*−*15*). However, the structural data are also compatible with an alternative mechanism in which His274 abstracts the hydroxyl proton from the substrate and promotes the transfer of a hydride ion from the α-carbon of the substrate to the FMN in a concerted mechanism (*16*). Thus, the exact mechanism of substrate oxidation by this enzyme family is still not completely resolved.

† This work was supported by an American Heart Association Postdoctoral fellowship (A.R.D.) and in part by a NIH Grant GM-54102 (B.M.).

* Address correspondence to the following author. E-mail: bmitra@med.wayne.edu. Phone: (313) 577-0040. Fax: (313) 577-2765.

[1] Abbreviations: $^{D}k_{cat}$, primary substrate kinetic isotope effects on k_{cat}; $^{D}k_{red}$, primary substrate kinetic isotope effect on k_{red}, the rate of FMN reduction; MDH, (*S*)-mandelate dehydrogenase.

10.1021/bi035349o CCC: $25.00
Published on Web 10/17/2003

In this study, we undertook a detailed kinetic characterization of the substrate oxidation and FMN reduction half-reaction. Using stopped-flow measurements, we observed a transient intermediate at low temperatures during both the forward and the reverse reactions. It appears to be a charge-transfer complex of oxidized FMN formed prior to its reduction. Oxidized FMN is electron-deficient and is known to form charge-transfer complexes with electron-rich donors (*17*). We present evidence that the charge-transfer donor is likely to be a carbanion intermediate and not a Michaelis complex with an anionic substrate. These results are compatible with a mechanism in which following substrate binding, a carbanion is generated that forms a charge-transfer complex with oxidized FMN. This complex disappears when the electrons are fully transferred to generate reduced FMN. The free energies of activation for both steps are similar, although the entropy of activation is significantly higher for the formation of the intermediate relative to its disappearance. This is the first report of a distinct transient intermediate during the course of the reductive half-reaction in this enzyme family and provides evidence against a concerted mechanism.

EXPERIMENTAL PROCEDURES

Materials

Reagents were purchased from commercial sources and were of the highest possible analytical grade. For the determination of the primary substrate kinetic isotope effect, [α-^{2}H]-(*S*)-mandelic acid was enzymatically prepared as described previously (*18*).

Methods

Enzyme Purification. *wt*MDH and the mutant enzymes were solubilized with detergent and purified using nickel-affinity chromatography as described earlier (*10*). Protein concentrations were estimated by measuring the free FMN released upon boiling the protein solutions for 5 min.

Steady-State and Presteady-State Kinetics. Steady-state activities were measured between 4 and 20 °C, in 0.1 M potassium phosphate, pH 7.5, containing 1 mg/mL bovine serum albumin, 1 mM phenazine methosulfate, and 100−150 μM dichloroindophenol, as described previously (*10*). Primary substrate kinetic isotope effects on k_{cat} and k_{red} ($^Dk_{cat}$ and $^Dk_{red}$, respectively) were measured using [α-^{2}H]-(*S*)-mandelate. Stopped-flow data were collected at different temperatures in 0.1 M potassium phosphate, under anaerobic conditions. The pH was 7.5 for all the studies, unless noted. Solutions were made anaerobic by saturating them with argon. Time-dependent spectra of the appearance and decay of the intermediate between 350 and 750 nm were recorded at different temperatures using a photodiode-array accessory connected to the stopped-flow spectrophotometer. In routine measurements, the appearance and decay of the intermediate was monitored at 560 nm. The data were fitted to single- or double-exponential fits, using the Pro/K software supplied by Applied Photophysics. Time-dependent spectra were also reconstructed from single-wavelength decay kinetics by recording the time-dependent change in absorbance at 5 nm intervals in the 300−700 nm range at 2 °C.

Reverse Reaction Catalyzed by wtMDH. To check whether MDH was capable of catalyzing the reverse reaction, 6 μM *wt*MDH in 0.1 M potassium phosphate, pH 7.5, was reduced with 50 μM (*S*)-mandelate at 20 °C under anaerobic conditions. A variety of other hydroxyacids were also used for reduction of the enzyme, notably 2-hydroxyoctanoate, which is a slow substrate as compared to (*S*)-mandelate, as well as sulfite, which forms a covalent adduct with the FMN in the active site (*10*). The fully reduced enzyme was restored to the oxidized state by the addition of excess benzoylformate or by admitting air to the reaction. In a separate experiment, *wt*MDH was reduced with sulfite; benzoylformate was then added to the reduced enzyme for a specified time. The decrease in benzoylformate concentration was quantitated by chemical derivatization with *o*-phenylenediamine (*19*). The reaction mixture was quenched with 2.5 mM *o*-phenylenediamine in 80% acetic acid and heated for 10 min at 50 °C, and the absorbance at 334 nm due to the formation of 3-phenylquinoxaline-2-ol was recorded. The amount of benzoylformate before and after reoxidation of reduced MDH was compared.

The reverse reaction was monitored in the stopped-flow spectrophotometer at 4 °C under anaerobic conditions as follows. One syringe was filled with 40 μM MDH reduced with either 10 mM 2-hydroxyoctanoate or 500 μM (*S*)-mandelate in 100 mM potassium phosphate, pH 7.5. The second syringe was filled with 20 mM benzoylformate and either 10 mM 2-hydroxyoctanoate or 500 μM (*S*)-mandelate in the same buffer.

Instrumentation. Steady-state kinetics was measured with a Varian (Cary 1E) spectrophotometer. Stopped-flow data were collected using an Applied Photophysics System (SX 18.MV) spectrophotometer equipped with a photodiode-array accessory.

RESULTS

Appearance of an Intermediate during the Course of the Reaction. Upon addition of the substrate, (*S*)-mandelate, to *wt*MDH, an intermediate was observed at 4 °C during the course of reduction of the enzyme-bound FMN. Figure 1A shows the difference spectra obtained in the 350−700 nm range in the stopped-flow spectrophotometer equipped with a diode-array accessory. The intermediate absorbs in the region 550−700 nm with a broad maximum centered around 575 nm and with a relatively low extinction coefficient. The time-scale of formation and decay of this intermediate, less than 10 ms, suggests that it is part of the catalytic reaction pathway. The maximal amount of the intermediate was observed at 4−6 ms. Additionally, Figure 1A clearly shows that the intermediate is formed before FMN is fully reduced; at 2.6 ms, only ∼12% of the FMN had been reduced whereas the intermediate had reached ∼40% of its maximal concentration. In other words, the intermediate occurs during the course of the first (FMN reductive) half-reaction. The spectrum of the intermediate in Figure 1A suggests that it is a charge-transfer complex of oxidized FMN. We examined the spectrum in the 300−400 nm region in more detail to rule out the possibility that the intermediate was a semiquinone of FMN. Figure 1B shows the reconstructed spectra obtained during the course of the reductive half-reaction from single-wavelength decay curves, generated at 5 nm intervals, in the region of 300−700 nm. Because of the limitations of the diode-array accessory, we could not measure real-time

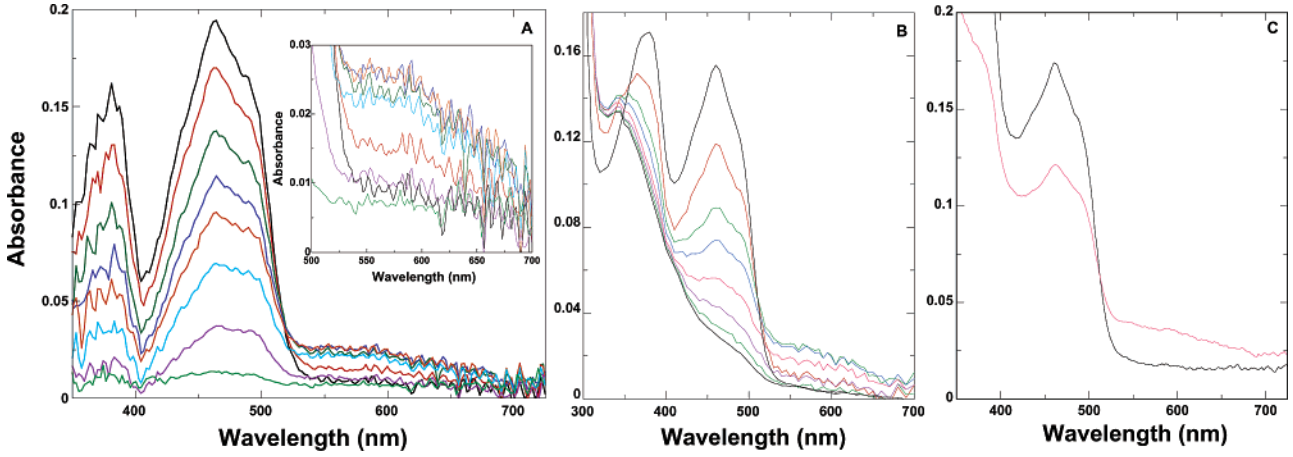

FIGURE 1: (A) Difference absorbance spectra recorded for *wt*MDH, in 100 mM potassium phosphate, pH 7.5 under anaerobic conditions at 4 °C. Spectra in descending order were recorded in a stopped-flow spectrophotometer equipped with a diode-array accessory 0.9, 2.6, 4.4, 6, 8, 11.4, 20, and 59 ms after the addition of 1 mM (*S*)-mandelate. The spectrum of the fully reduced enzyme, recorded at 700 ms, was subtracted from each spectrum shown. The inset is an expanded view showing the appearance and decay of the intermediate between 500 and 700 nm. (B) Spectra reconstructed from single-wavelength decay curves for *wt*MDH after the addition of 1 mM (*S*)-mandelate, in 100 mM potassium phosphate, pH 7.5 under anaerobic conditions at 2 °C. Decay curves were obtained at 5 nm intervals in the wavelength range of 300−700 nm. Spectra in descending order are that of the oxidized enzyme, after 3.25, 6.25, 9.25, 15.25, 27.25, and 50.25 ms, and completely reduced enzyme. (C) Comparison of the spectrum of oxidized *wt*MDH (black) and the simulated spectrum of the charge-transfer intermediate (pink). The spectrum of the intermediate was simulated from the continuous spectra obtained with the photodiode-array accessory and the Pro/K software.

spectra of the intermediate below 350 nm. The reconstructed spectra clearly show that the intermediate has no absorbance in the 300−400 nm region characteristic of a neutral or anionic semiquinone. It is to be noted that *wt*MDH stabilizes the anionic semiquinone (A. R. Dewanti and B. Mitra, unpublished observations). Thus, the data in Figure 1A,B rule out the possibility that the intermediate could be a semiquinone of the flavin. It is likely to be a charge-transfer complex of FMN that is formed before its reduction.

From the time-dependent spectra obtained using the photodiode-array accessory, the actual spectrum of the charge-transfer complex could be simulated using the model, $E_{ox} \rightarrow I \rightarrow E_{red}$ and the Pro/K software. Figure 1C shows a simulated spectrum of the intermediate. The intermediate retains 68% of the absorbance of oxidized FMN at 460 nm and also has long-wavelength absorbance with a low extinction coefficient above 550 nm.

Temperature Dependence of the Intermediate Formation. The intermediate could only be observed at low temperatures. The data in Figure 2A,B show the changes in absorbance at 460 and 560 nm at two different temperatures, upon the addition of 1 mM (*S*)-mandelate to *wt*MDH. The data at 4 °C could be fitted well to two-exponential equations; using a three-exponential equation did not significantly improve the fit for either the 460 or the 560 nm data. The model used to describe the data was

$$E{\cdot}FMN_{ox} + S \xrightarrow{k_1} I \xrightarrow{k_2} E{\cdot}FMN_{red}$$

where $E{\cdot}FMN_{ox}$ is oxidized MDH, I is the intermediate, and $E{\cdot}FMN_{red}$ is fully reduced MDH. The fit of the 560 nm data at 4 °C yielded rate constants of 420 ± 8 s^{-1} for the formation of the intermediate (k_1) and 119 ± 1 s^{-1} for its disappearance (k_2). From the unconstrained fit of the 460 nm data, we obtained rate constants of 254 ± 4 for k_1 and 40 ± 1 s^{-1} for k_2; the smaller rate constant together with its amplitude accounted for about 4% of the data. Interestingly, the 460 nm data could be fitted quite well to a two-exponential equation when either or both rate constants were constrained to be those obtained from the 560 nm fit. These results confirm that the formation and decay of the intermediate at 560 nm coincides with the overall reduction of FMN as monitored by the decrease in absorbance at 460 nm.

When the reaction of *wt*MDH with (*S*)-mandelate was monitored at room temperature, the intermediate was formed within the dead-time of the stopped-flow instrument. In other words, although free oxidized or fully reduced MDH has no absorbance above 560 nm, upon addition of substrate at room temperature, the intermediate with its characteristic low absorbance above 560 nm was formed immediately (Figure 2A,B). At 20 °C, the decay at both 460 and 560 nm could be fitted to a two-exponential equation, with rate constants of 514 ± 8 ms^{-1} and 46 ± 3 s^{-1} obtained for the 460 nm data and rate constants of 457 ± 6 and 24 ± 4 s^{-1} obtained for the 560 nm data. In both cases, the smaller rate constants together with their amplitude accounted for less than 1% of the decay. The rate constants obtained at 460 and 560 nm and 514 and 457 s^{-1}, respectively, are in reasonable agreement with each other, especially given the noise in the 560 nm data at early time points. These rate constants describe the decay of the intermediate (k_2). Thus, we can conclude that at room temperature, the breakdown of the intermediate coincides with the overall reduction of FMN. This provides additional proof that the charge-transfer intermediate was formed with oxidized FMN.

We next investigated the temperature dependence of the two rate constants, k_1 and k_2, by monitoring the changes in absorbance at 560 nm at different temperatures. As shown in Figure 3A, k_1 increases rapidly with temperature, such that at temperatures ≥10 °C, the intermediate is formed within the dead time of the instrument, and k_1 could not be reliably determined. The disappearance of the intermediate, described by k_2, is a slower process relative to its formation.

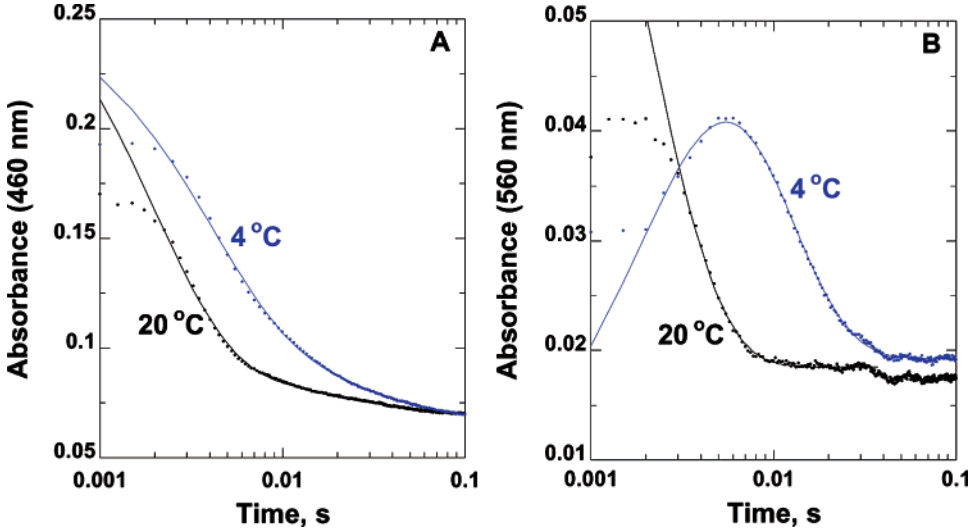

FIGURE 2: Changes in absorbance at (A) 460 and (B) 560 nm obtained for *wt*MDH following the addition of 1 mM (*S*)-mandelate (final concentration) at 4 and 20 °C. Reaction conditions were as described in Figure 1A. The lines represent two-exponential fits to the data starting from 2 ms.

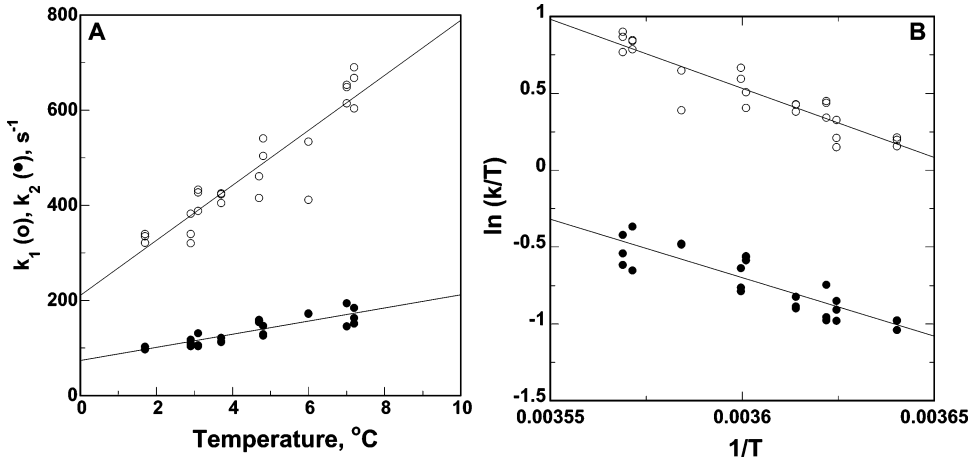

FIGURE 3: Temperature dependence of the rate of formation, k_1 (○), and rate of disappearance, k_2 (●), of the intermediate. Reaction conditions were as described in Figure 1A.

The data in Figure 3A were replotted as ln(k/T) versus 1/T (Figure 3B) and fitted to a linear form of the Eyring equation

$$k = (k_B/h)T \exp(\Delta S^{\ddagger}/R) \exp(-\Delta H^{\ddagger}/RT)$$

$\Delta S^{\ddagger}$ and $\Delta H^{\ddagger}$ were calculated from the intercept and slope of the plot, respectively. The activation energy, $\Delta G^{\ddagger}$, was calculated at 25 °C from the relationship

$$\Delta G^{\ddagger} = \Delta H^{\ddagger} - T\Delta S^{\ddagger}$$

At 25 °C, $\Delta H^{\ddagger}$ and $\Delta S^{\ddagger}$ for k_1 were 74.9 kJ/mol and 76.5 J/(K mol), respectively, for (*S*)-mandelate as substrate (Table 2). The corresponding $\Delta H^{\ddagger}$ and $\Delta S^{\ddagger}$ for k_2 were 63.5 kJ/mol and 25.2 J/(K mol), respectively. From these values, we obtained $\Delta G^{\ddagger}$ values of 52.1 and 55.9 kJ/mol for k_1 and k_2, respectively, at 25 °C.

Substrate Dependence of Intermediate Formation. The physiological substrates of *wt*MDH and its homologues are hydroxyacid anions. Therefore, we considered the possibility that the enzyme-bound substrate forms the intermediate complex with FMN, before any reaction occurs. We tested a variety of substrates and inhibitors for their ability to form the intermediate. (*R*)-Mandelate and 1-phenylacetate, anionic competitive inhibitors of (*S*)-mandelate, failed to form the intermediate (*10*). No intermediate was observed with anionic

Table 1: Steady-State and Presteady-State Kinetic Parameters for *wt*MDH with (*S*)-Mandelate[a]

	4 °C	20 °C
k_{cat} (s^{-1})	134 ± 3	360 ± 8
K_m (mM)	0.11 ± 0.00	0.12 ± 0.01
$^{D}k_{cat}$	2.0	2.2
k_{red} (s^{-1})		402 ± 16
K_d (mM)		0.19 ± 0.03
$^{D}k_{red}$		2.1
k_1 (s^{-1})	398 ± 26	
k_2 (s^{-1})	121 ± 10	457 ± 6
$^{D}k_1$	3.0	
$^{D}k_2$	1.9	2.1

[a] Steady-state assays were in 0.1 M potassium phosphate, pH 7.5, containing 1 mg/mL bovine serum albumin, 100−150 μM dichloroindophenol, and 1 mM phenazine methosulfate. Presteady-state measurements were in 0.1 M potassium phosphate, pH 7.5. k_{red} is the rate of FMN reduction monitored at 460 nm. Since there are two components to k_{red} at 4 °C, k_1 and k_2 (measured by monitoring absorbance changes at 560 nm) are reported instead of k_{red}. At 20 °C, k_1 was too fast to measure. $^{D}k_{cat}$, $^{D}k_{red}$, $^{D}k_1$, and $^{D}k_2$ are primary substrate kinetic isotope effects on k_{cat}, k_{red}, k_1, and k_2, respectively.

Table 2: Activation Energy Parameters of the Intermediate for the Reaction with (*S*)-Mandelate[a]

	$\Delta H^{\ddagger}$ (kJ mol^{-1})	$\Delta S^{\ddagger}$ (J mol^{-1} K^{-1})	$\Delta G^{\ddagger}$ (at 25 °C) (kJ mol^{-1})
k_1	74.9 ± 6.7	76.5 ± 6.7	52
k_2	63.5 ± 7.2	25.2 ± 2.9	56

[a] The values of $\Delta H^{\ddagger}$ and $\Delta S^{\ddagger}$ were calculated using data from Figure 3B. $\Delta G^{\ddagger}$ was calculated at 25 °C.

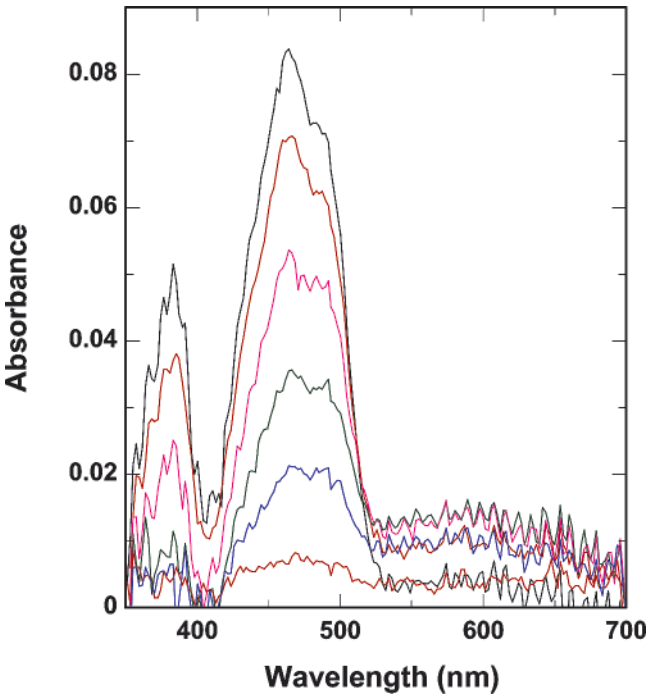

FIGURE 4: Difference absorbance spectra recorded for 20 μM *wt*MDH, in 100 mM potassium phosphate, pH 7.5 under anaerobic conditions at 4 °C after the addition of 2 mM (*R*,*S*)-4-chloromandelate. Spectra, in descending order, were recorded in a stopped-flow spectrophotometer equipped with a diode-array accessory 0.9, 2.6, 4.4, 8, 15, and 50 ms after substrate addition. The spectrum of the reduced enzyme, recorded at 100 ms, was subtracted from each spectrum shown.

substrates that have low activities with *wt*MDH, 2-hydroxyhexanoate, and 2-hydroxyoctanoate (*10*). However, the ring-substituted mandelate analogues, (*R*,*S*)-4-chloro and (*R*,*S*)-4-bromomandelates that have relatively high activities with *wt*MDH, were able to form the intermediate (Figure 4). Interestingly, neutral ester analogues of mandelic acid and ethyl and methyl mandelates, which have k_{cat} values approaching that of (*S*)-mandelate, were also able to form the intermediate (Dewanti, A., Xu, Y., and Mitra, B., manuscript in preparation).

Dependence of the Rates of Intermediate Formation and Decay on Substrate Concentration. To determine the dependence of the rate of formation and disappearance of the intermediate on the substrate concentration, we measured absorbance changes at 560 nm at 4 °C for different (*S*)-mandelate concentrations. The 560 nm data were fitted to a two-exponential equation to generate k_1 and k_2. Figure 5 shows a plot of the two rate constants as a function of the substrate concentration. The values for k_1 and k_2 at saturating substrate concentrations were 398 ± 26 and 121 ± 10 s^{-1}, respectively (Tables 1 and 2). Substrate concentrations at half-saturation values of k_1 and k_2 were 0.19 ± 0.04 and

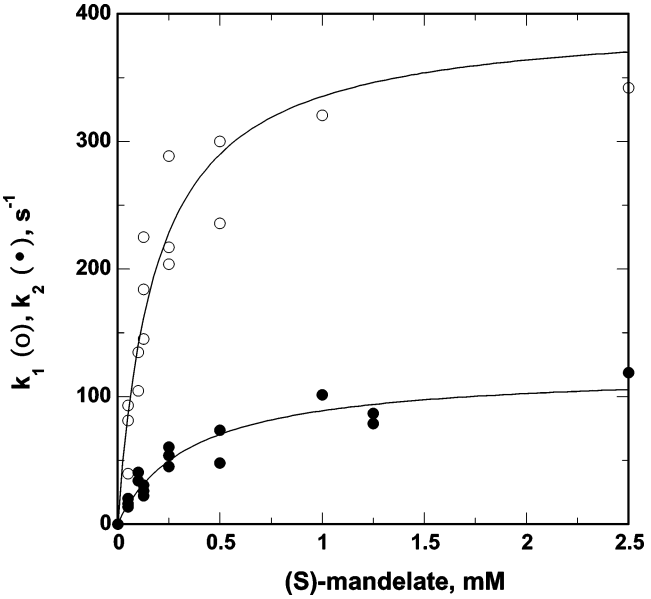

FIGURE 5: Dependence of the rate of formation, k_1 (○), and the rate of disappearance, k_2 (●), of the charge-transfer intermediate on the concentration of (*S*)-mandelate in 100 mM potassium phosphate, pH 7.5 under anaerobic conditions at 4 °C. The data were fitted to a hyperbolic equation.

0.36 ± 0.08 mM, respectively. For the steady-state reaction at 4 °C, a k_{cat} of 134 ± 3 s^{-1} and a K_m of 0.11 mM were obtained.

We also measured the primary substrate kinetic isotope effects on the rates of formation and breakdown of the intermediate (Figure 6). It is clear from Figure 6B that the substrate kinetic isotope effect is more pronounced on the rate of formation of the intermediate as compared to its breakdown. The decay at 560 nm at 4 °C for saturating concentrations of ^{2}H-(*S*)-mandelate (2.5 mM) was fitted to a two-exponential equation, with rate constants of 137 ± 3 and 63 ± 1 s^{-1}. Comparing the rates obtained at 560 nm for ^{1}H-(*S*)-mandelate and ^{2}H-(*S*)-mandelate, we can calculate an isotope effect of 3.0 ± 0.2 for the formation and 1.9 ± 0.1 for the decay of the intermediate (Tables 1 and 2). The $^D k_{cat}$ for *wt*MDH at 4 °C, measured in steady-state assays, is 2.0 (Table 1); at 20 °C, the $^D k_{cat}$ has been shown to be 2.2 (*10*).

pH Dependence of Intermediate Formation. MDH has a broad pH optimum for its steady-state activity; the pH profile is a bell-shaped curve. The activity decreases below pH 5.5 and above pH 9.5 (*13*). The intermediate could be observed at pH 6.7, 7.5, and 9.1; both k_1 and k_2 were similar at all three pHs. Unfortunately, MDH was somewhat unstable when incubated at pHs below 6 and above 9.5; therefore, stopped-flow data could not be measured at the pHs at which the steady-state parameters change substantially.

MDH Catalyzes the Reverse Reaction. Reduced *wt*MDH is capable of catalyzing the reverse reaction, the reduction of a ketoacid to an (*S*)-α-hydroxyacid. Figure 7A shows that *wt*MDH, reduced with limiting quantities of (*S*)-mandelate, is capable of being reoxidized by air or by high concentrations of the reaction product, benzoylformate, under anaerobic conditions. That the reverse reaction is indeed occurring was ascertained as follows. Following the reduction of MDH with sulfite and its subsequent reoxidization by benzoylformate, the concentration of benzoylformate was quantitated by derivatizing with *o*-phenylenediamine. The decrease in

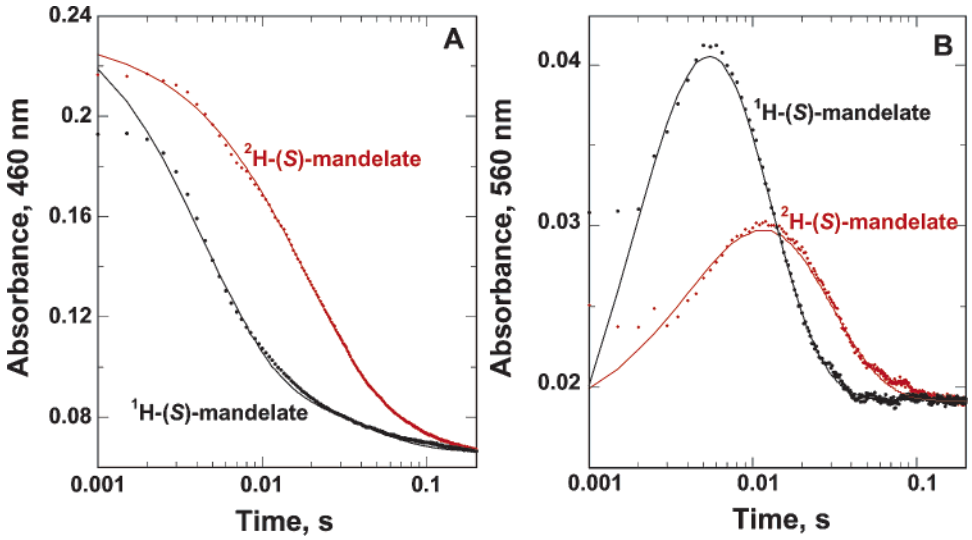

FIGURE 6: Changes in absorbance at 4 °C at (A) 460 and (B) 560 nm obtained for *wt*MDH following the addition of 2.5 mM (*S*)-^{1}H-mandelate (black) or 2.5 mM (*S*)-^{2}H-mandelate (red). Reaction conditions were as described in Figure 1A. The lines represent two-exponential fits to the data starting from 2 ms.

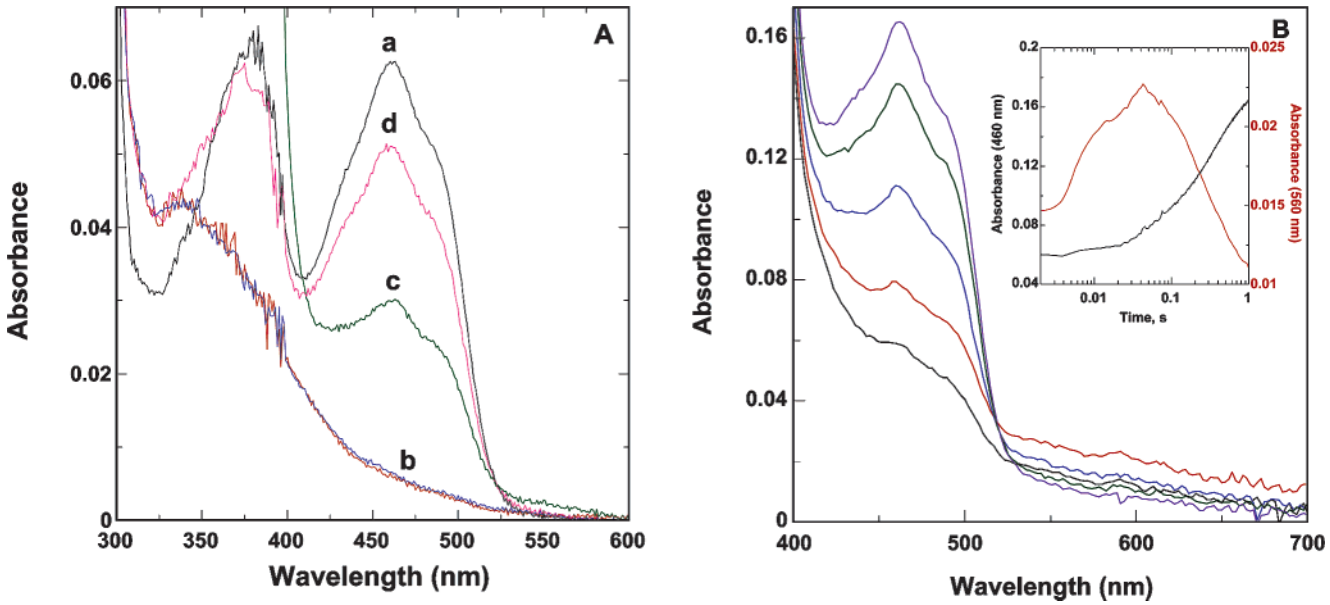

FIGURE 7: (A) Reoxidation of reduced *wt*MDH by 2-ketoacids. Oxidized *wt*MDH (6 μM) (trace a, in black) was reduced with 50 μM (*S*)-mandelate in 100 mM phosphate, pH 7.5, at room temperature under anaerobic conditions (trace b, blue and red). The reduced enzyme was then oxidized by adding 15 mM benzoylformate under anaerobic conditions (trace c, green) or by admitting air to the medium (trace d, magenta). (B) Absorbance spectra recorded for 40 μM *wt*MDH reduced with 10 mM 2-hydroxyoctanoic acid, in 100 mM potassium phosphate, pH 7.5 under anaerobic conditions at 4 °C, after the addition of 50 mM benzoylformate. Spectra, in ascending order, were recorded in a stopped-flow spectrophotometer equipped with a diode-array accessory 3.8, 45, 200, 500 ms, and 1 s after benzoylformate addition.

the amount of benzoylformate corresponded to the amount of reduced enzyme used in the reaction.

Appearance of the Intermediate during the Reverse Reaction. The transient intermediate could be observed at 4 °C during the reoxidation of reduced MDH by benzoylformate in the stopped-flow spectrophotometer (Figure 7B). In this experiment, MDH was reduced with 10 mM 2-hydroxyoctanoate and then mixed with high concentrations (50 mM) of benzoylformate. The intermediate could be observed as the reduced flavin was reoxidized during the reverse reaction. The inset to Figure 7B shows the changes in absorbance at 460 and 560 nm during the reoxidation reaction. This experiment shows that the intermediate is formed both in the forward and the reverse directions of the MDH reaction. The intermediate was not observed when the ketoacid corresponding to a slow hydroxyacid substrate was used for the reoxidation reaction, for example, 2-ketooctanoate, 2-ketohexanoate, or 2-phenylpyruvic acid (*13*). However, the intermediate was observed when MDH was reduced by either a slow substrate, 2-hydroxyoctanoate, or a fast substrate, (*S*)-mandelate.

Intermediate Formation for Mutants of MDH at Residue Arg277. We have previously shown that Arg277 plays a critical role in binding the anionic substrate and in stabilizing a negatively charged intermediate during catalysis (*13*). The charge-conserved mutation R277K is a fairly active protein although with a substantially weaker affinity for the substrate; however, all other mutations at Arg277 result in large decreases in activity. The ability of R277K and R277G to form the intermediate during the course of the reaction was

Scheme 1

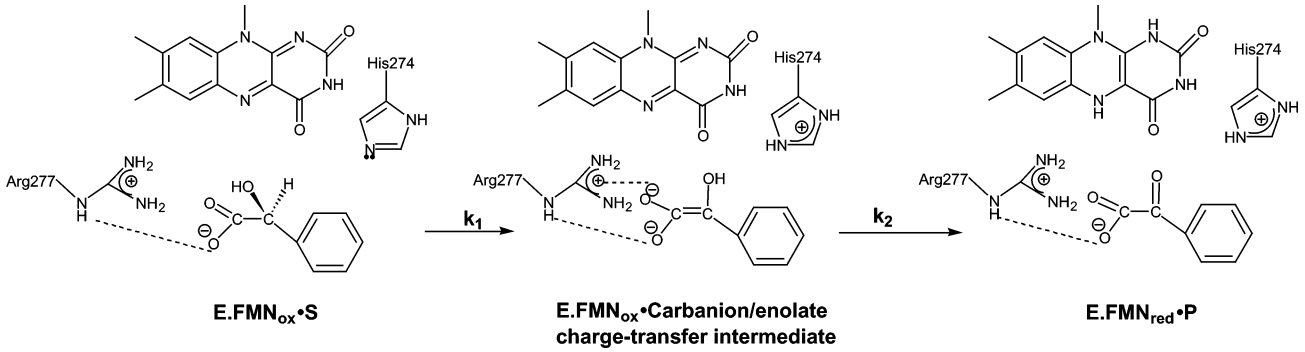

tested. The intermediate could not be observed for either mutant during the reduction of MDH. Figure 8 shows difference spectra obtained for R277K after the addition of (*S*)-mandelate. It is to be noted that R277K has a k_{red} of 67 s^{-1} and a K_d of 5.2 mM, while R277G has a k_{red} of 0.3 s^{-1} and a K_d of 17.5 mM; in contrast, *wt*MDH has a k_{red} of 402 s^{-1} and a K_d of 0.2 mM at 20 °C (*13*−*14*).

DISCUSSION

The reaction mechanism of MDH and homologous α-hydroxyacid oxidases and dehydrogeneases is believed to either involve a doubly negative carbanion/enolate intermediate, which transfers its electrons to the flavin (Scheme 1), or a direct transfer of a hydride ion from the negatively charged substrate to the flavin. In the latter case, we do not expect to observe a distinct intermediate. To elucidate the mechanism further, we undertook a detailed characterization of the first reductive half-reaction in this study. At 20 °C, the decrease in absorbance of FMN as a result of its reduction occurred without the appearance of any intermediate; however, the data at very early time points suggested that the decrease in absorbance at 460 nm might be biphasic. When we measured the kinetic parameters of MDH at 4 °C, we observed a distinct but very short-lived intermediate. The spectrum of this intermediate suggests that it is a charge-transfer complex of oxidized FMN. At 20 °C, formation of the intermediate was too fast to measure; however, its breakdown coincided with the reduction of FMN.

Charge-transfer complexes of oxidized FMN are well-documented; the FMN in Old Yellow Enzyme forms such complexes with the phenolate anion (*17*). In sulfhydryl oxidase from egg white, a thiolate to oxidized FAD charge-transfer complex has been observed, as also a NADH to oxidized FAD complex in NADH peroxidase (*20*, *21*). A charge-transfer complex attributed to an enolate intermediate donor and oxidized FAD acceptor was also observed during the course of the reaction for medium chain acyl-CoA dehydrogenase at low temperatures when a dienoyl CoA derivative was used as substrate (*22*). Oxidized FAD in D-amino acid oxidase forms charge-transfer complexes with substituted benzoates (*23*). In each of these cases, the donor involved in the charge-transfer complex is an electron-rich anion, and the acceptor is the electrophilic oxidized FMN.

Charge-Transfer Complex Is Not Due to an Enzyme−*Substrate Complex*. Since the substrate in the MDH reaction is the anion of a hydroxyacid, we first investigated whether the bound substrate could form a charge-transfer complex with oxidized FMN prior to any bond-making or -breaking steps. The intermediate was not observed with anionic competitive inhibitors or with slow anionic substrates such as 2-hydroxyoctanoate but only observed with (*S*)-mandelate and analogues that have high k_{cat} values. Thus, the charge-transfer donor is not the substrate itself but an intermediate that is formed after substrate binding but prior to FMN reduction. This conclusion is also supported by our observation that the charge-transfer intermediate was observed with neutral ester analogues of mandelic acid and ethyl and methyl mandelates, which have k_{cat} values approaching that of (*S*)-mandelate but extremely weak affinities relative to the hydroxyacid anion (Dewanti, A. R., Xu, Y., and Mitra, B., manuscript in preparation). The possibility that only aromatic molecules could form the charge-transfer complex was ruled out by the observation that the binding of 1-phenylacetate, (*R*)-mandelate, and 1-phenylpyruvate failed to produce the intermediate. As expected from an intermediate that is formed fairly early in the reaction pathway immediately following substrate binding, it has a dependence on the substrate concentration.

Free Energy Parameters for the Intermediate. At both 20 and 4 °C, the kinetic parameters of the FMN reductive reaction are similar to those for the overall steady-state reaction (Tables 1 and 2). Therefore, the rate-limiting step(s) in the overall reaction occurs in the first, reductive half-reaction. However, within the FMN reductive reaction, there is clearly more than one step that is rate limiting in the case of *wt*MDH. The kinetic parameters of the charge-transfer intermediate at 4 °C show that the rate of its formation is similar to its rate of disappearance; the former is 3−4-fold faster than the latter. This is also true at 20 °C; k_1 is 3−4-fold larger than k_2, as calculated from extrapolation of the data in Figure 3A. Activation energy parameters calculated for the intermediate show that its disappearance has a much lower change in entropy relative to its formation; this suggests that the intermediate resembles the product more than the substrate. Thus, the intermediate must be the enolate anion, in which the α-carbon is planar as in the product ketoacid and not tetrahedral as in the substrate hydroxyacid. The free energies of activation of both steps are quite similar, ∼52−56 kJ/mol, although the $\Delta G^{\ddagger}$ for the breakdown of the intermediate is slightly higher, as expected from a 3−4-fold lower value for k_2. Since the two rates are quite similar, the overall reaction rate depends on both k_1 and k_2, rate constants that describe the formation and disappearance of the charge-transfer complex.

Kinetic Isotope Effects Suggest that the Charge-Transfer Complex Is Due to the Carbanion Intermediate. The nature

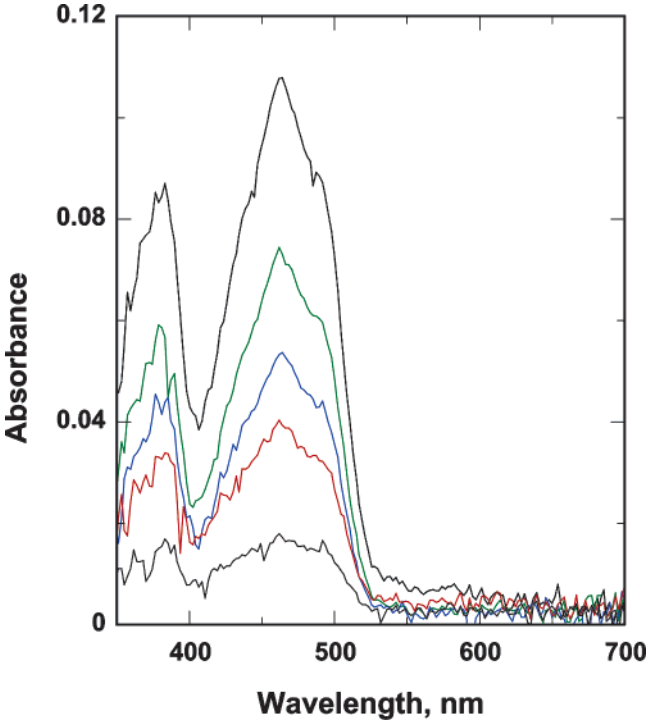

FIGURE 8: Difference absorbance spectra recorded for 15 μM R277K after the addition of 10 mM (*S*)-mandelate in 100 mM potassium phosphate, pH 7.5 under anaerobic conditions at 4 °C. Spectra, in descending order, were recorded in a stopped-flow spectrophotometer equipped with a diode-array accessory 2.6, 31, 61, 100, and 200 ms after substrate addition. The spectrum of the fully reduced enzyme, recorded at 700 ms, was subtracted from each spectrum shown.

of the charge-transfer donor is revealed by kinetic isotope effect data on k_1 and k_2 at 4 °C (Tables 1 and 2). The rate of formation of the intermediate, k_1, has a larger isotope effect than k_2, the rate of its decay. This suggests that formation of the charge-transfer intermediate coincides with the step where the α-carbon−hydrogen bond of the substrate is broken. Since the charge-transfer donor must be electron-rich, but is not the substrate anion itself, it is most likely the carbanion/enolate intermediate generated by the base-catalyzed abstraction of the α-carbon by His274 (Scheme 1). The charge-transfer complex is therefore formed between the enolate as donor and the oxidized FMN as acceptor. According to this scheme, the disappearance of the intermediate should not have a large isotope effect. Indeed, the isotope effect is smaller; the reason it is not one is probably due to the fact that the two rates are quite similar to one another and therefore difficult to separate. It is to be noted that the overall $^{D}k_{cat}$ at 4 °C is less than that on k_1, as expected given that both k_1 and k_2 contribute to the overall rate of the reaction.

pH Dependence of the Intermediate Formation. Charge-transfer complexes are normally dependent on the pH of the medium. The kinetic parameters, k_1 and k_2, for the formation and decay of the intermediate were similar at pH 6.5, 7.5, and 9.1. We have shown earlier that the steady-state activity of MDH has a broad pH optimum; the activity starts to decrease below pH 5.5 and above pH 9.5 (*13*). The decrease below pH 5.5 is due to protonation of the active site base His274, which is responsible for the formation of the carbanion (*12*). The decrease above pH 9.5 is due to deprotonation of Arg277, which can no longer stabilize the carbanion (Scheme 1) (*13*). Since the charger-transfer complex appears to be formed with the carbanion as donor, it is not surprising that its kinetic parameters are unchanged at the pH values at which the carbanion remains stable. Unfortunately, since MDH is unstable at pHs above 9.5 and below 6, we could not directly determine if the intermediate would be destabilized at these pH extremes, especially above pH 9.5, where Arg277 gets deprotonated and is unable to stabilize the carbanion.

Role of Arg277 in Stabilizing the Intermediate. The positive charge at Arg277 plays a critical role in stabilizing a negatively charged intermediate during the reaction (*13*). The R277K mutant has a ~6-fold lower k_{cat} relative to *wt*MDH, while the R277G mutant is an extremely poor enzyme. The substrate kinetic isotope effect obtained for R277K, 4.6−5.1, suggested that its 6-fold lower activity was the result of a negative effect on the carbanion formation/stabilization step (*13*). In agreement with this conclusion, we could not detect the charge-transfer intermediate for the two Arg277 mutants at 4 °C. This lends further support to the idea that the charge-transfer complex is indeed due to the formation of the carbanion. In fact, now that it is evident that there are two rate-limiting steps of similar activation energies for the *wt*MDH reaction, corresponding to formation and breakdown of the carbanion/enolate intermediate, the 6-fold decrease in overall k_{cat} for R277K possibly corresponds to a much higher decrease in the value of k_1 since k_1 is 3−4-fold faster than k_2 for *wt*MDH. The larger isotope effect data for R277K of 4.6−5.1 implies that for R277K the step described by the rate constant, k_1, has become completely rate limiting.

Charge-Transfer Complex Is Not Due to a Reduced FMN Product Complex. Charge-transfer complexes between reduced flavin and enzyme-bound product have been observed for many flavoproteins, including MDH homologues and related enzymes. A stable charge-transfer complex of reduced FMN and product, which was not part of the reaction pathway, was observed with lactate monooxygenase, an α-hydroxyacid oxidizing enzyme belonging to the same family as MDH (*24*). For D-amino acid oxidase, a reduced FAD product ketoacid charge-transfer complex was also observed during the course of the reaction (*25*). Incidentally, during oxidation of nitroethane by D-amino acid oxidase, when the preformed carbanion of nitroethane was added to the enzyme, the reaction proceeded through three distinct steps: a charge-transfer complex of oxidized FAD and the carbanion in a noncovalent complex, reduction of FAD, and a charge-transfer complex of reduced FAD and the product (*25*). In other words, in addition to the charge-transfer complex formed by D-amino acid oxidase with reduced FAD and ketoacid product, another charge-transfer complex is observed with the oxidized FAD when the substrate is added as an anion. The usual substrate for D-amino acid oxidase is not anionic. It is to be noted that for both lactate monooxygenase as well as for D-amino acid oxidase with certain substrates, the product has a high affinity for the reduced enzyme, whereas for *wt*MDH, the affinity of the product for reduced enzyme is 600-fold lower than that of the substrate for the oxidized enzyme (Sukumar, N., Dewanti, A. R., Mitra, B., and Mathews, F. S., manuscript submitted).

Interestingly, a charge-transfer complex that is part of the reaction pathway was observed for another enzyme homolo-

gous to MDH, lactate oxidase from *Aerococcus viridans* (*3*). This was ascribed to a reduced FMN and product complex. The reasoning was that it was also observed when the product, pyruvate, was added to the reduced enzyme. It was assumed that the rate of the reverse reaction was zero; in other words, lactate oxidase was completely unable to catalyze the reoxidation of the reduced FMN by pyruvate. However, no rationale or proof was offered as to why the reverse reaction cannot occur for this enzyme, especially given the fact that the reverse reaction (transhydrogenation) has been nicely demonstrated for a homologous enzyme, flavocytochrome b_2 from *S. cerevisiae* (*26*). Our results had already demonstrated that the charge-transfer complex was clearly due to the oxidized flavin. However, we wanted to ascertain whether it could be observed during the course of the reverse reaction, and indeed, whether the reverse reaction occurs in MDH or not. Our results show that the MDH reaction is reversible. Reduced MDH can be slowly oxidized by air or rapidly by the addition of the product ketoacid, benzoylformate. Given the poor affinity of the product, benzoylformate, for reduced MDH, a high concentration of benzoylformate was necessary to drive the reverse reaction. As expected for a microscopically reversible reaction, the charge-transfer complex was also observed at low temperatures during the course of the reverse reaction. This confirms that the intermediate is indeed part of the true reaction pathway and can be observed in both the forward and the reverse directions.

Conclusions. In this paper, we have shown that the substrate oxidation/FMN reduction half-reaction in *wt*MDH proceeds through the formation of a distinct transient intermediate. This intermediate appears to be a charge-transfer complex of an electron-rich donor and oxidized FMN. The intermediate is extremely short-lived, and its formation can only be observed at low temperatures. The rates of its formation and disappearance are similar; the latter is 3−4-fold slower. Isotope effect measurements suggest that the electron-rich donor may be a carbanion/enolate intermediate. Thus, the MDH reaction has two rate-limiting steps of similar activation energies, both occurring in the first half-reaction: the formation and disappearance of the charge-transfer intermediate, which correspond to the formation and breakdown of the carbanion/enolate intermediate. Enzymes homologous to MDH such as lactate oxidase and flavocytochrome b_2 that use aliphatic hydroxyacid substrates appear to have a single rate-limiting step, as indicated by the full isotope effect on both the k_{cat} and the k_{red}. The reason for the different behavior of MDH is likely to be the result of its unusual substrate. A carbanion of (*S*)-mandelate is expected to be more stable than one from lactate since the negative charge can be delocalized on the aromatic ring. However, the α-carbon atom of mandelate is more sterically constrained relative to that in lactate. If electron transfer from the carbanion occurs via a covalent adduct formation between its α-carbon and FMN as has been proposed, this step is likely to require a higher activation energy in MDH than in the homologous enzymes (*27*, *28*).

ACKNOWLEDGMENT

We are indebted to Profs. Dave Ballou and John Gerlt for early help with this work and for pointing us toward the existence of a reaction intermediate at low temperatures.

REFERENCES

1. Tsou, A. Y., Ransom, S. C., Gerlt, J. A., Buechter, D. D., Babbitt, P. C., and Kenyon, G. L. (1990) *Biochemistry 29*, 9856−9862.
2. Diep Le, K. H., and Lederer, F. (1991) *J. Biol. Chem. 266*, 20877−20881.
3. Maeda-Yorita, K., Aki, K., Sagai, H., Misaki, H., and Massey, V. (1995) *Biochimie 77*, 631−642.
4. Lindqvist, Y. (1989) *J. Mol. Biol. 209*, 151−166.
5. Xia, Z., and Mathews, F. S. (1990) *J. Mol. Biol. 212*, 837−863.
6. Lindqvist, Y., Branden, C.-I., Mathews, F. S., and Lederer, F. (1991) *J. Biol. Chem. 266*, 3198−3207.
7. Sukumar, N., Xu, Y., Gatti, D. L., Mitra B., and Mathews, F. S. (2001) *Biochemistry 40*, 9870−9878.
8. Bruice, T. C. (1980) *Acc. Chem. Res. 13*, 256−262.
9. Ghisla, S., and Massey, V. (1989) *Eur. J. Biochem. 181*, 1−17.
10. Lehoux, I. E., and Mitra, B. (1999) *Biochemistry 38*, 5836−5848.
11. Reid, G. A., White, S., Black, M. T., Lederer, F., Mathews, F. S., and Chapman, S. K. (1988) *Eur. J. Biochem. 178*, 329−333.
12. Lehoux, I. E., and Mitra, B. (1999) *Biochemistry 38*, 9948−9955.
13. Lehoux, I. E., and Mitra, B. (2000) *Biochemistry 39*, 10055−10065.
14. Xu, Y., Dewanti, A. R., and Mitra, B. (2002) *Biochemistry 41*, 12313−12319.
15. Muh, U., Williams, C. H., and Massey, V. (1994) *J. Biol. Chem. 269*, 7994−8000.
16. Mattevi, A., Vanoni, M. A., Todone, F., Rizzi, M., Teplyakov, A., Coda, A., Bolognesi, M., and Curti, B. (1996) *PNAS 93*, 7496−7501.
17. Abramovitz, A. S., and Massey, V. (1976) *J. Biol. Chem. 251*, 5327−5336.
18. Landro, J. A., Kallarakal, A. T., Ransom, S. C., Gerlt, J. A., Kozarich, J. W., Neidhart, D. J., and Kenyon, G. L. (1991) *Biochemistry 30*, 9274−9281.
19. Li, R., and Kenyon, G. L. (1995) *Anal. Biochem. 230*, 37−40.
20. Hoober, K. L., and Thorpe, C. (1999) *Biochemistry 38*, 3211−3217.
21. Crane, E. J., Parsonage, D., Poole, L. B., and Claiborne, A. (1995) *Biochemistry 34*, 14114−14124.
22. Wang, W., Fu, Z., Zhou, J. Z., Kim, J.-J. P., and Thorpe, C. (2001) *Biochemistry 40*, 12266−12275.
23. Massey, V., and Ganther, H. (1965) *Biochemistry 4*, 1161−1173.
24. Lockridge, O., Massey, V., and Sullivan, P. A. (1972) *J. Biol. Chem. 247*, 8097−8106.
25. Porter, D. J. T., Voet, J. G., and Bright, H. J. (1973) *J. Biol. Chem. 248*, 4400−4416.
26. Urban, P., Alliel, P. M., and Lederer, F. (1983) *Eur. J. Biochem. 134*, 275−281.
27. Ghisla, S., and Massey, V. (1989) *Eur. J. Biochem. 181*, 1−17.
28. Ghisla, S., and Massey, V. (1990) *Flavins and Flavoproteins*, pp 124−130, Walter de Gruyter, Berlin, New York.

BI035349O